13 December 1996

ELSEVIER

Chemical Physics Letters 263 (1996) 385–392

CHEMICAL PHYSICS LETTERS

Isomerization versus hydrogen exchange reaction in the HNC ⇌ HCN conversion

D. Talbi, Y. Ellinger

Groupe d'Astrochimie Quantique, Laboratoire de Radioastronomie, Ecole Normale Supérieure et Observatoire de Paris, 24 rue Lhomond, 75005 Paris, France

Received 23 August 1996; in final form 11 October 1996

Abstract

For the HNC/HCN interconversion we show that the push–pull hydrogen exchange reaction H + CNH ⇌ HCNH ⇌ HCN + H is favoured over internal isomerization; the formation of H_2CN or CNH_2 followed by rearrangement to HCNH and subsequent elimination are more energy demanding processes. Both push–pull forward and reverse reactions present activation barriers. However, the activation energy on the H + CNH entrance channel (4.2 ± 1.0 kcal/mol) is four times smaller than on the HCN + H path. As a consequence, it can be anticipated that there will be a range of temperatures where the H + CNH reaction will be efficient while the reverse HCN + H process is still inhibited. This process, much less endothermic than internal isomerization, should become an important path for HNC/HCN conversion with increasing temperature in star forming regions.

1. Introduction

There are two contexts in which to consider the evolution of the HCN/HNC pair of isomers; one is terrestrial and the other is related to space chemistry. On earth, gaseous hydrogen cyanide (HCN) is an important intermediate in the combustion reactions of hydrocarbon flames containing a nitrogen source. Because atomic hydrogen is also a major component of flames, Bair and Dunning have done a systematic examination of processes in which H and HCN species react with each other [1]. By contrast, the HNC isomer, a compound of much lower stability, has hardly been considered because of its rarity on earth which makes it interesting only for academic studies. In this sense, the HCN ⇌ HNC system has sometimes been taken as a model for unimolecular reactions and the corresponding barrier to the isomerization investigated [2,3].

From an astrophysical point of view, the situation is different. In the chemical model of the formation of interstellar HCN and HNC, it is assumed that these two isomers are equally formed through the electronic dissociative recombination of the $HCNH^+$ [4] ion. HNC has effectively been observed in various interstellar clouds to be as abundant as HCN. More puzzling are observations that the abundance ratio HNC/HCN varies from one source to another in apparent relation with temperature. In order to explain these variations, the first process which comes to mind is isomerization of HNC to HCN, which, inefficient at low temperature, would become relevant at high temperature. However, because this reaction requires an activation energy of ≅ 29

PII S0009-2614(96)01253-5

kcal/mol [3], much too high to be overpassed in the interstellar conditions, it will not contribute to the HNC depletion. Another mechanism has to be found in order to consume HNC in which the forward reaction HNC → HCN is efficient when temperature increases while the backward reaction HNC ← HCN is still inhibited. The reaction hypothesized to fulfill these requirements [5] is

$$H + CNH \rightarrow HCN + H$$

which implies atomic hydrogen, ubiquitous in the interstellar medium. This assumption, though appealing, has never been confirmed in the laboratory because extreme difficulties in the realization of the experiments. In this Letter, we present an alternative approach based on quantum chemical theory. To assess whether or not hydrogen addition competes with the hydrogen exchange process, we also considered the formations of H_2CN and H_2NC as well as their isomerizations to HCNH.

2. Computational details

An extensive mapping of the H + HNC ⇌ HCNH ⇌ HCN + H potential energy surface of $^2A'$ symmetry has been realized, including electron correlation at the MP2/6-31G(d,p) level of theory. The geometries of all the stationary points (reactants, intermediates and transition states) have been optimized in C_s symmetry. The character of each stationary point on

Table 1
MP2/6-31G(d,p) geometries, harmonic vibrational frequencies zero-point energies and MP3/6-311 + + G(d,p) geometries

Molecule		Frequencies	Zero-point energy
H	$E = 0.498232$		
HCN [a]	$r(CH) = 1.064$ (*1.066*)	$\Pi_i = 737$	
$^1\Sigma_g^+$	$r(CN) = 1.176$ (*1.150*)	$\Sigma_g = 2045, 3536$	9.600
	$E = -93.174366$		
HNC	$r(NH) = 0.997$ (*0.996*)	$\Pi_i = 495$	
$^1\Sigma_g^+$	$r(CN) = 1.186$ (*1.168*)	$\Sigma_g = 2045, 3894$	9.773
	$E = -93.142322$		
$(HCN–H)_{TS}$	$r(NH) = 1.418$ (*1.461*)	$a' = i2246, 621, 821, 2553, 3580$	
($^2A'$)	$r(CH) = 1.065$ (*1.067*)	$a'' = 963$	11.83
	$r(CN) = 1.157$ (*1.151*)		
	$\angle(CNH) = 124.93$ (*122.18*)		
	$\angle(NCH) = 190.15$ (*188.58*)		
	$E = -93.63225\ 1$		
$(HNC–H)_{TS}$	$r(NH) = 0.997$ (*0.996*)	$a' = i1096, 368, 481, 2074, 3888$	
($^2A'$)	$r(CH) = 1.744$ (*1.784*)	$a'' = 540$	10.18
	$r(CN) = 1.187$ (*1.171*)		
	$\angle(CNH) = 188.84$ (*184.66*)		
	$\angle(NCH) = 122.56$ (*120.38*)		
	$E = -93.630043$		
HCNH	$r(NH) = 1.014$ (*1.016*)	$a' = 839, 1226, 2519, 3135, 3627$	
($^2A'$)	$r(CH) = 1.095$ (*1.098*)	$a'' = 993$	17.09
	$r(CN) = 1.214$ (*1.215*)		
	$\angle(CNH) = 122.14$ (*119.64*)		
	$\angle(NCH) = 123.99$ (*125.99*)		
	$E = -93.686470$		

For a definition of the structural parameters see Fig 1. Distances are given in ångström, angles in degrees and energies in hartree. Frequencies are given in cm^{-1} and zero-point energies in kcal/mol. MP3/6-31 + + G(d,p) optimized geometries are reported in brackets.
[a] Experimental values: $\Pi_i = 713$; $\Sigma_g = 2097, 3312$ (Ref. [7]). Theoretical frequencies should be scaled by 0.969 before comparison with experiment. Zero-point energies have been scaled by 0.969.

the surface (minimum or saddle-point) was assessed by computing the harmonic vibrational frequencies. The results are given in Table 1 and Fig. 1.

In order to access a better description of the energetics of the hydrogen exchange reaction, the relative energies of the five stationary points on the [HCNH] surface have been computed using higher levels of theory. The basis sets have been improved from split valence polarized 6-31G(d,p) to triple split-valence to which diffuse orbitals have been added together with two and then three sets of polarization functions, namely 6-311 + + G(3df,2pd)

Table 2
MP2/6-31G(d,p) geometries, harmonic vibrational frequencies and zero-point energies

Molecule		Frequencies	Zero-point energy
H_2CN	r(CH) = 1.091	a_1 = 1461, 2086, 3124	
($^2B_2$)	r(CN) = 1.221	b_2 = 979, 3201	16.66
	∠NCH = 121.54°	b_1 = 1175	
	E = −93.694241		
H_2NC	r(NH) = 1.016	a_1 = 1472, 1680, 3498	16.69
($^2B_2$)	r(CN) = 1.302	b_2 = 1045, 3595	
	∠(CNH) = 122.85°	b_1 = 757	
	E = −93.651455		
$(H_2CN)_{TS}$	r(CH) = 1.639	a' = i*1772*, 667, 1125, 2500, 3522	12.13
($^2A'$)	r(CH) = 1.068	a'' = 946	
	r(CN) = 1.152		
	∠(NCH) = 108.08°		
	∠(HCN) = 159.63°		
	E = −93.635869		
$(H_2NC)_{TS}$	r(NH) = 1.461	a' = i*2538*, 704, 1153, 2006, 3750	11.40
($^2A'$)	r(NH) = 1.006	a'' = 615	
	r(CN) = 1.204		
	∠(CNH) = 123.48		
	∠(HNC) = 137.73		
	E = −93.601945		
$(HC/H\backslash N)_{TS}$	r(CH) = 1.187	a' = i*2242*, 1103, 2651, 2796, 3112	13.67
($^2A'$)	r(CH) = 1.098	a'' = 210	
	r(CN) = 1.240		
	∠(NCH) = 63.59°		
	∠(HCN) = 135.76°		
	E = −93.622785		
$(HN/H\backslash C)_{TS}$	r(NH) = 1.149	a' = i*2149*, 1071, 1630, 2675, 3113	11.76
($^2A'$)	r(NH) = 1.038	a = i*213*	
	r(CN) = 1.291		
	∠(CNH) = 66.61°		
	∠(HNC) = 133.40°		
	E = −93.582012		
$(HCN)_{TS}$	r(XH) = 1.148	a' = i*1312*, 2107, 2803	6.80
($^1A'$)	r(CN) = 1.196		
	∠(CXH) = 76.49°		
	E = 93.086109		

For definition of structural parameters see Fig 2. Distances are given in ångströms, angles in degrees, energies in hartree, frequencies in cm^{-1} and zero-point energies in kcal/mol. Theoretical frequencies should be scaled by 0.969 before comparison with experiment. Zero-point energies have been scaled by 0.969.

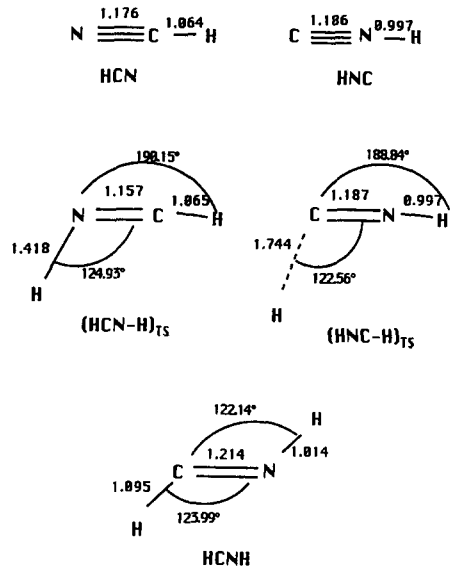

Fig. 1. Stationary points on the [HCNH] potential energy surface. Distances are in ångström and angles in degrees.

and 6-311 + + G(3df,3pd). In so doing, we reach a flexibility in the single determinant representation which approaches the Hartree–Fock limit. Calculations using these basis sets have been carried out at the SCF, MP2, MP3 and MP4 levels for MP2/6-31G(d,p) optimized geometries. A similar series of calculations has been performed for the MP3/6-311 + + G(d,p) optimized structures reported in Table 1 in order to evaluate the uncertainty of the energy profile with the level of wavefunction used for the geometry optimization.

All along the H + CNH ⇌ HCNH ⇌ HCN + H reaction path, a careful check of the spin eigenvalues has been done with particular attention to the transition states whose positions are critical for assessing the feasibility of the reaction. The $(HNC–H)_{TS}$ wavefunction is not significantly spin contaminated, the value for $\langle S^2 \rangle$ being 0.78 compared to 0.75 for a pure doublet. For the $(HCN–H)_{TS}$ structure, the situation is slightly worse, the highest value for $\langle S^2 \rangle$ being 0.88. Looking for a better computational protocol, we performed coupled cluster (CCSDT) and quadratic configuration interaction (QCISD) assuming with Fortunelli [6] that unrestricted coupled cluster wavefunctions are less spin-contaminated than their many-body perturbation theory counterparts. Test studies performed on the $(HCN–H)_{TS}$ structure showed that the $\langle S^2 \rangle$ values obtained at these levels of wave functions ($\langle S^2 \rangle = 0.99$) are worse than those found for our previous UMP4 calculations. Møller–Plesset perturbation theory was therefore retained for all calculations.

Transition states and stable structures resulting from the addition of atomic hydrogen to HNC (hereafter $(H_2NC)_{TS}$, H_2NC) and HCN (hereafter $(H_2CN)_{TS}$, H_2CN) have then been optimized at the same MP2/6-31G(d,p) level. The isomerizations of H_2NC and H_2CN to the stable HCNH trans structure have also been considered and the corresponding transition states $(HN/H\backslash C)_{TS}$ and $(HC/H\backslash N)_{TS}$ determined. The results are reported in Table 2 and Fig. 2.

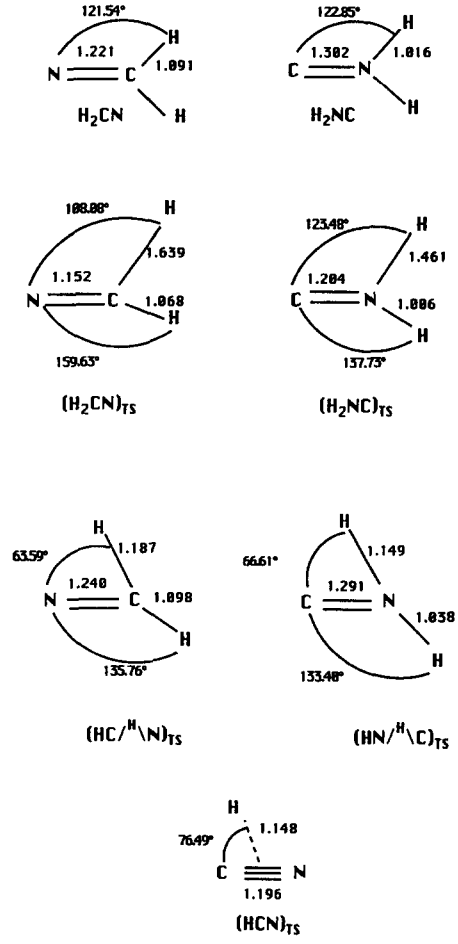

Fig. 2. Stationary points on the $[H_2NC/H_2CN]$ potential energy surface. Distances are in ångström and angles in degrees.

Table 3
MP4/6-311++G(3df,3pd) energies calculated at the MP2/6-31G(d,p) geometries

Molecule	State	E	E_0
H	^2S	−0.499818	−0.499818
$(HCN)_{TS}$	$^2A'$	−93.247862	−93.237024
HNC	$^1\Sigma_g$	−93.301518	−93.286219
HCN	$^1\Sigma_g$	−93.326044	−93.310469
$(HN/H\backslash C)_{TS}$	$^2A'$	−93.756133	−93.737394
$(H_2NC)_{TS}$	$^2A'$	−93.773557	−93.755393
$(HC/H\backslash N)_{TS}$	$^2A'$	−93.794090	−93.772296
$(HNC-H)_{TS}$	$^2A'$	−93.795959	−93.779732
$(HCN-H)_{TS}$	$^2A'$	−93.801827	−93.782978
$(H_2CN)_{TS}$	$^2A'$	−93.805463	−93.786125
H_2NC	$^2B_2$	−93.821473	−93.794878
HCNH	$^2A'$	−93.855372	−93.828130
H_2CN	$^2B_2$	−93.862370	−93.835820

Energies in hartree are calculated at the MP4/6-311++U(3df,3pd)//MP2/6-31U(d,p) level. E_0 includes scaled (by 0.969) MP2/6-31G(d,p) zero-point vibrational energies.

For a quantitative discussion, all electronic energies have been determined at the MP4 level using the 6-311 + + G(3df,3pd) basis set (Table 3). Zero-point vibrational energies have been computed from the harmonic frequencies of Tables 1 and 2. In order to account for the correlation still missing at this level of wavefunction all frequencies have been scaled by an empirical factor of 0.969 deduced from direct comparison of the experimental IR spectra of HCN [7] to our computed one. In order to account for possible artefacts when comparing isolated species to interacting ones (basis set superposition error) energies were corrected, when indicated, using the counterpoise technique [8,9].

All calculations reported here have been performed by means of the GAUSSIAN 92 computer code [10].

3. Results and discussion

All the reaction schemes considered for the HNC/HCN conversion are reported in Fig. 3. In addition to the isomerization path, the reaction profile of the exchange process H + CNH ⇌ HCNH ⇌ HCN + H (hereafter trans-addition elimination) has been drawn from the energies corrected for the zero point energy contribution and BSSE artefacts. The relative positions of the various intermediates H_2NC, H_2CN and corresponding transition states $(H_2NC)_{TS}$, $(H_2CN)_{TS}$, $(HN/H\backslash C)_{TS}$ and $(HC/H\backslash N)_{TS}$ are included on the surface. For these energies, only zero-point energy corrections have been considered since BSSE can be neglected in view of the large energy differences involved in the corresponding processes. The corresponding reaction profile will be referred to as cis-addition elimination.

A cursory examination of the MP4/6-311++G(3df,3pd)//MP2/6-31G(d,p) reaction pathways visualized in Fig. 3 shows HNC to be 15.2 kcal/mol above the HCN ground state. This number can be compared to the 14.6 kcal/mol obtained by Pearson et al.[2] and to the value of 16.0 kcal/mol obtained by DeFrees et al. [3] in large scale CI calculations.

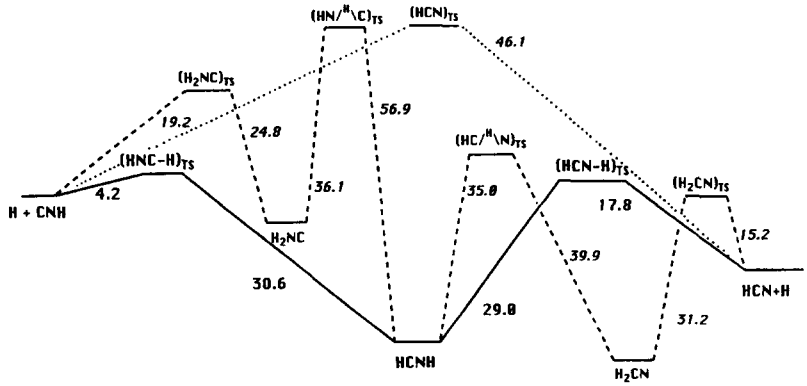

Fig. 3. Energy profiles for the HNC/HCN conversion: (– – –) trans-addition–elimination, (- - -) cis-addition–elimination, (· · ·) isomerization.

Our barrier for isomerization of HNC to HCN is 30.8 kcal/mol in excellent agreement with the 29 kcal/mol obtained in the CI treatment. Such an energy is clearly not available in the interstellar medium and the attention will be focused on the two remaining pathways.

3.1. Trans addition–elimination

The results of Table 4 show the energy convergence with respect to increasing electronic correlation with the order of perturbation theory (from MP2 to MP3 and MP4); the SCF wavefunction is totally inadequate even if close to the Hartree–Fock limit.

The known statement that MP3 calculations yield reliable geometries [11] is verified here. Our MP3 optimized values (in brackets in Table 1.) are accurate within 1%, as illustrated by the known structures of HCN (CH = 1.065 Å; CN = 1.153 Å) [7] and HNC (NH = 0.986 Å; CN = 1.173 Å) [12]. However our previous experience on IR spectra have shown that MP3 wavefunctions are not well adapted for the vibrational calculations needed in the present case to retrieve the zero-point energy corrections. To evaluate the error made by considering the MP2 optimized geometry, a comparison of the MP4 calculations obtained using MP2/6-31G(d,p) and MP3/6-311 + + G(d,p) optimized geometries has been done. The energy differences appear to be smaller than 0.3 kcal/mol, which puts an upper limit on the error possibly related to the uncertainty in the MP2 equilibrium geometries. Table 3 also indicates that extending the basis set from a 6-311 + + G(3df,2pd) to 6-311 + + G(3df,3pd) has similar consequences on the relative energies (the variations are less than 0.2 kcal/mol). Further improvement in the correlation treatment is not known to modify the energies significantly. A last type of uncertainty comes from the evaluation of the zero-point vibrational energy corrections. The scaling factor used in the present work has been transferred from HCN. Assuming an error (certainly overestimated) of 100 cm^{-1} (0.3%) for the other stationary point at the same level of theory introduces an uncertainty of 0.2 kcal/mol. The level of calculations is of high enough quality in the basis set and correlation treatment that we can reasonably

Table 4
Energies (kcal/mol) relative to HNC + H for the H + HNC ⇌ HCN + H trans addition–elimination

Molecule		SCF	MP2		MP3		MP4		MP4 [a]
		(a)	(a)	(b)	(a)	(b)	(a)	(b)	
H + CNH	E	0.0	0.0	0.0	0.0	0.0	0.0	0.0	0.0
	E_0	0.0	0.0	0.0	0.0	0.0	0.0	0.0	0.0
$(HNC–H)_{TS}$	E	8.72	5.07	4.99	4.09	4.03	3.44	3.37	3.65
	E_0	9.29	5.65	5.57	4.67	4.61	4.02	3.95	4.23
	best	**estimate** [b]	**4.2 ± 1.0**						
HCNH	E	−29.8	−31.5	−31.7	−35.8	−36.0	−33.7	−33.9	−33.9
	E_0	−22.5	−24.0	−24.2	−28.3	−28.5	−26.2	−26.4	−26.4
	best	**estimate**	**−26.4 ± 1.0**						
$(HCN–H)_{TS}$	E	5.88	2.80	2.62	0.41	0.22	−0.12	−0.31	−0.02
	E_0	8.05	5.03	4.85	2.64	2.45	2.11	1.92	2.21
	best	**estimate** [b]	**2.6 ± 1.0**						
HCN + H	E	−8.40	−17.5	−17.5	−13.0	−13.0	−15.4	−15.4	−15.4
	E_0	−8.23	−17.3	−17.3	−12.8	−12.8	−15.2	−15.2	−15.2
	best	**estimate**	**15.2 ± 1.0**						

E are computed at the optimized MP2/6-31G(d,p) geometries with: (a) 6-311 + + G(3df,2pd) basis set; (b) 6-311 + + G(3df,3pd)basis set.
[a] MP4 are energies computed with the 6-311 + + G(3df,3pd) basis set at the MP3/6-311 + + G(d,p) optimized geometries.
E_0 includes scaled MP2/6-31U(d,p) zero-point vibrational energies.
[b] The best estimated energies include the BSSE corrections which increased the relative energies of $(HNC–H)_{TS}$ and $(HCN–H)_{TS}$ by respectively 0.27 and 0.64 Kcal/mol.

assign, for the forward reaction, an error bar (certainly overestimated) of 1.0 kcal/mol in the energy differences obtained at the MP4 level for MP2 optimized structures. This error bar might be slightly higher for the calculated activation barrier on the HCN + H side because of the higher spin contamination of the $(HCN–H)_{TS}$ wavefunction.

Our best estimate of the potential surface as given in Table 4 shows that both hydrogen approaches, towards the nitrogen side (HCN + H) and towards the carbon side (HNC + H), lead to repulsive surfaces with no stable long-range complexes. Our best estimations of the barriers are

4.2 ± 1.0 kcal/mol on the HNC + H entrance channel,

17.8 ± 1.0 kcal/mol on the HCN + H entrance channel.

The corresponding transition states are positioned such that $(HNC–H)_{TS}$ is 1.6 kcal/mol higher than $(HCN–H)_{TS}$. It should be noted that the $(HCN–H)_{TS}$ transition state relaxes directly to the trans-HCNH structure while previous studies have found [1] that this same $(HCN–H)_{TS}$ state first gives a cis-HCNH structure before relaxing to the more stable trans structure by going through another transition state that we were not able to characterize at the perturbation level of theory.

3.2. Cis addition–elimination

A second reaction pathway is presented in Fig. 3. This implies cis additions on carbon or nitrogen leading to H_2CN or CNH_2, the former being the most stable stationary point on the surface. The H + CNH entrance channel presents an activation barrier of 19.2 kcal/mol on the way to CNH_2, i.e. four times higher than the barrier which opposes the direct formation of HCNH. This structure can however be reached by displacement of one hydrogen atom from nitrogen to carbon; the activation barrier on this process is 30.5 kcal/mol above the initial products. On the reverse channel, the addition of H to HCN to form H_2CN presents an activation barrier of 15.2 kcal/mol, which is 2.6 kcal/mol lower than that found on the direct path to HCNH. This common point on the surface can also be reached from H_2CN if the 39.9 kcal/mol barrier to the hydrogen shift can be overpassed.

The part of the present surface corresponding to the addition of hydrogen to the carbon of HCN is in qualitative agreement with that reported by Bair et al. [1]. Some differences appear when comparing in detail the relative energies of H_2CN, $(H_2CN)_{TS}$, HCNH and $(HC/H\backslash N)_{TS}$. The reason can be found in the theoretical level used at that time by the authors (POL-CI) to calculate their energies, which is now known to give qualitative but not quantitative energy balances. Moreover, the geometries, optimized at the MCSCF level, present overestimated bond lengths as noticed by the authors themselves when comparing their results to calculations incorporating more correlation effects. Finally, the fact that their zero-point energies were calculated also at the MCSCF level introduces one more source of energy discrepancy.

4. Concluding remarks

The present study on the HNC + H ⇌ HCN + H system brings some new information about the interconversion mechanisms between HNC and HCN. The conversion of HNC to HCN through hydrogen trans addition–elimination appears to be the most probable mechanism. It requires only 4.2 kcal/mol whereas direct isomerization through a hydrogen shift from nitrogen to carbon would need almost eight times more energy. The cis addition–elimination path through CNH_2 followed by internal rearrangement to HCNH before elimination presents an activation barrier of an order of magnitude higher. A similar conclusion can be drawn for the conversion of HCN to HNC. The hydrogen trans-addition–elimination is more efficient since it only needs 17.8 kcal/mol, whereas the direct isomerization costs 46 kcal/mol. The cis-addition–elimination path through H_2CN, although passing through the most stable intermediate on the surface requires more activation energy. Thus we can state that the hydrogen exchange reaction is the efficient process for the HNC/HCN isomerization. MCSCF calculations designed to analyze the difference in the reactivity of the two isomers show that it can be traced to the difference in their electronic structures. Careful examination of the

natural orbitals shows that HNC has a carbenic structure whose most easily accessible electrons are those of the lone pair orbital. By contrast, the accessible electrons for HCN are those of the π bonding orbitals of the triple bond, the nitrogen lone pair orbital being deep below. Breaking the π bonding electrons ($\cong$ 2.5 eV) to form the NH bond, requires much more energy than decoupling the carbene lone pair to form the CH bond (the S–T separation is only $\cong$ 0.5 eV).

Two important consequences follow from the *push–pull* energy profile which have to be outlined here.

(i) The fact that the activation energy for the HNC + H reaction is lower than the activation energy for the HCN + H one means that less energy is needed to overcome the repulsive barrier in the first process. As a direct consequence, there is a domain of temperatures where the direct reaction will consume HNC whereas the reverse one is still inhibited.

(ii) The relative position of the transition states has a consequence that, when the $(HNC–H)_{TS}$ transition complex is reached, there is no further barrier on the path to dissociation to H + HCN.

In the astrophysical context, the present study indicates that at temperatures high enough to overcome an activation energy of about 4.2 kcal/mol ($\cong$ 2000 K) the HNC molecule is transformed into HCN whose abundance increases accordingly, while the back transformation to HNC is not likely to happen because of an energy barrier of 17.8 kcal/mol. The formation of any intermediate (HCNH, H_2CN, H_2NC) requires a third body and/or internal relaxation; such a process should have little importance under the conditions of the interstellar medium but might be significant in planetary atmospheres.

Acknowledgements

Part of the calculations reported in this Letter were supported by the 'Institut du Développement et des Ressources en Informatique Scientifique' which is gratefully acknowledged.

References

[1] R.A. Bair and H. Dunning, J. Chem. Phys. 92 (1985) 2280.
[2] P.K. Pearson and H.F. Schaefer III, J. Chem. Phys. 62 (1975) 350.
[3] D.J. DeFrees, G.H. Loew and A.D. McLean, Astrophys. J. 257 (1982) 376.
[4] D. Talbi and Y. Ellinger to be submitted.
[5] P. Schilke, C.M. Walmsley, P. Gineau des Forets, E. Roueff, D.R. Flower and S. Guilloteau, Astron. Astrophys. 256 (1992) 595.
[6] A. Fortunelli, Int. J. Quantum Chem. 52 (1994) 97.
[7] G Herzberg, Electronic spectra and electronic structures of polyatomic molecules (Van Nostrand, New York, 1966).
[8] S.F. Boys and F. Bernardi, Mol. Phys. 19 (1970) 553.
[9] B. Liu and A.D. McLean, J. Chem. Phys. 59 (1973) 4557.
[10] M.J. Frisch, G.W. Trucks, M. Head-Gordon, P.M.W. Gill, M.W. Wong, J.B. Foresman, B.G. Johnson, H.B. Schlegel, M.A. Robb, E.S. Replogle, R. Gomperts, J.L. Andres, K. Raghavachari, J.S. Binkley, C. Gonzalez, R.L. Martin, D.J. Fox, D.J. DeFrees, J. Baker, J.J.P. Stewart and J.A. Pople Gaussian 92, Revision E.2 (Gaussian, Pittsburgh, PA) (1992).
[11] D.J. DeFrees and A.D. McLean, J. Chem. Phys. 82 (1985) 333.
[12] M.D. Harmony, V.W. Laurie, R.L. Kuckzowski, R.H. Schwendeman, D.A. Ramsay, F.J. Lovas, W.J. Lafferty and A.G. Maki, J. Phys. Chem. Ref. Data, 8 (1979) 619.